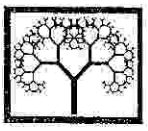

© 1994, CIVIL-COMP Ltd, Edinburgh, Scotland
B.H.V. Topping and M. Papadrakakis (Editors),
Advances in Structural Optimization, 119-130

OPTIMAL SHAPE OF DAMS SUBJECT TO EARTHQUAKES

L.M.C. Simoes and J.A.M. Lapa
Departmento de Engenharia Civil, Faculdade de Ciencias e Tecnologia
University of Coimbra, Portugal

Abstract

The purpose of this paper is to show an application of the maximum entropy formalism to the shape optimization of dams subject to seismic loading. The structural system is discretized by the finite element method. The dynamic response analysis is computed by modal analysis or step by step integration procedures. Emphasis is placed on the derivation of the sensitivity analysis equations done by the analytic method and based on the dynamic analysis procedure to be employed. The earthquake response includes dam-reservoir and dam-foundation interactions. The shape optimization of a concrete gravity dam is posed as a multiobjective optimization with goals of minimum volume of concrete, stresses and maximum safety against overturning and sliding. By using the maximum entropy formalism it is shown that a Pareto solution may be found indirectly by the unconstrained optimization of a scalar function. The validity and effectiveness of the proposed technique is examined by means of a concrete gravity dam.

In Memorian

JOSÉ SIMÕES

1. Introduction

The design of continuum structures such as dams presents a unique task. Such structures are fundamentally configuration optimization problems where the external geometry of the structure is to be determined. The optimal design problems can be stated in a mathematical programming form with geometric design variable representing coordinates of the nodes or boundaries of elements. It should be emphasized that the geometric constraints imposed on the continuum structure are such that the procedures of scaling are not appropriate. Moreover, maximum stresses appear in certain sections, but the majority of the critical sections is not fully stressed under any load combination at the optimum. Each design stage of the iterative process presented here involves: (1) The analysis of an initial or trial design by finite element analysis; (2) Use of sensitivity analysis and approximation concepts to formulate the performance constraints as explicit linear functions of design variables; (3) optimization by means of an efficient optimization algorithm to obtain a better solution. The new design then becomes the trial design for the next design iteration and the process is continued until the change in design over a number of successive design stages is less than some specified tolerance.

The finite element techniques, taking into account plane strains, soil interaction, thermal stresses, etc. are now current practice for dam design and can be used in the optimization process. A feature of the problem is that there may be few significant design variables and the model is rather simplified by using a coarse finite-element mesh. One of the first robust optimization algorithms developed for the solution of linear problems was the Simplex. It was natural that researchers attempted to use this algorithm for nonlinear problems by linearizing the constraints and objective function about a trial design (Zienckiewicz and Campbell, [1]). Penalty function methods have been applied by Ramakrishnan and Francavilla [2] and by Vitiello [3] to the shape optimization of hollow gravity and solid gravity dams respectively. In both papers a static two dimensional finite element analysis module is used. The first application of shape optimization for arch dam design was carried out by Rajan using membrane shell theory. This method ignores foundation elasticity and boundary stresses and considers a single loading condition. More recent results for the three-dimensional shape optimization of arch dams subjected to static loading reported so far use as a method of obtaining solutions a sequential linear programming algorithm associated with either 8 node (Wasserman,[4]) or 20 node Ricketts [5] and Zienckiewicz [1] isoparametric elements. All of these papers concern the static behaviour of dams.

However, the stresses in gravity dams due to standard design loads have little resemblance to the dynamic response to earthquake ground motion. The standard requirements do not predict large tensile stresses associated with cracking that may occur during earthquakes. The main source of this discrepancy lies in ignoring the dynamic characteristics of earthquake motions of dams in specifying the earthquake forces. The analysis of the response of concrete gravity dams to seismic loading has been the subject of intensive investigation in the last two decades. Particularly notable is the research conducted by Chopra and his co-workers who arrived at important conclusions regarding the significance of a number of factors contributing to the response. Firstly, the seismic coefficient is very small compared to the ordinates of acceleration spectra for intense earthquake motions in the period range typical of concrete gravity dams. Secondly, the assumption that the seismic coefficient is uniform over the height ignores the dependence of the seismic coefficient distribution on the vibration mode shapes of the dam [6]. The interactions between the dam and impounded water and of water compressibility were found to have substantial effects during both horizontal and vertical ground motions. It has been demonstrated that the traditional design procedures have serious limitations because they are based on unrealistic assumption: Rigid dam and incompressible water. Further, the absorption of hydrodynamic pressure waves into the alluvium and sediment deposited at the bottom of reservoirs and the interaction between the dam and underlying flexible foundation rock were established as factors that should be considered in the detailed response history analysis procedure for the two-dimensional finite element idealization of gravity-dams monoliths Chopra et al.[7] and Fenves et al.[8]. More recent work indicates that solid sediment do not influence the response of the dam to horizontal ground motion significantly, wether the foundation is rigid or flexible. Perhaps the most pronounced effects is the response of the dam rigid foundation to vertical ground motions: the peaks become finite and are appreciably shifted primarily as a result of the decrease in water depth because of the sediment [9]

The ground motion history from an earthquake is considered in this work as support excitation for the structure. Step-by-step integration procedures and modal analysis are used for dynamic response analysis. The earthquake response includes dam-reservoir and dam-foundation interaction. The design loads for dams include water pressure in addition to the hydrostatic pressures associated with earthquakes. Hydrodynamic pressure on vertical rigid dams subjected to harmonic ground motions was first solved analytically by Westergaard in 1933. The solution procedure adopted in this paper considers the general solution of the wave equation in an expanded form that satisfies all the boundary conditions except one at the upstream face of the dam. The unknown coefficient of the expansion are obtained by imposing boundary conditions at this upstream face of the dam using least squares.

The sensitivities of the response quantities with respect to the design variables for use in the optimization method are of primary concern. The calculation of the sensitivity of structural response to changes in the design variables is often the major computational cost of the the optimization process. Therefore it is important to have efficient algorithms to evaluate the sensitivities. Two general approaches are used for computing sensitivities: differentiation of the continuum equations followed by discretization, and the reverse approach of discretization followed by differentiation. Variational and discrete sensitivity calculations in transient structural analysis were reported by Haftka et al.[10]. The semianalytic method belonging to the latter class will be used here. The choice of methods has important accuracy and implementation implications. The semi-analytical method is based on finite difference evaluations of the derivatives of the stiffness matrix and the load vector is used in this work. For shape design variables the truncation error associated with with the finite difference approximations of the derivative of the stiffness matrix may be substantial. However, the pseudo-load applied to the structure to produce the sensitivity field is a reasonable displacement field for the structure and its boundary conditions preventing this source of inaccuracies.

In the past most effort in the field of optimum design of structures have been focused on solving for static loads. Little consideration has been given to the area of dynamic structural response with most of the work being done to control frequency constraints. Ref.[11-12] are representative of the papers dealing with frequency constraints and aeroelastic flutter constraints. There has been some work with dynamic loading, most often for time-variant loads which are sinusoidal or some form of pseudo earthquake loading Cassis and Schmit [13]. Dynamic response constraints differ from frequency constraints in that they have a time parametric form. A type of dynamic input that is of particular importance to the structural engineer is that produced by earthquakes. This optimization problem always involves great difficulties since displacements, velocities and accelerations are in general implicit non-linear functions of the design variables. Moreover dynamic structural design optimization problems often lead to disjoint feasible regions in the design space. For problems in which some of the constraints are quite expensive to calculate, bounds can be developed for the constraints that replace the original constraints in the optimization problem and help to provide bounds on the optimum solution. One such example was given by Mills-Curran and Schmidt [14]. In that application, they developed time-dependent upper bounds for dynamic displacement and stress constraints which are valid for lightly damped systems away from resonant forcing conditions.

The cost of a dam is a function of such components as area of formwork, volume of excavation and volume of concrete. The latter component is often a dominant factor in the determination

of cost. The constraints consist of nodal displacements, stresses and in the case of gravity dams safety against sliding and overturning. If a linear system is assumed, the non-linear dynamic analysis could be avoided by considering another set of constraints: bound(s) on the natural frequency(ies). However, the step-by-step integration technique is more suitable to model nonlinear behaviour that may occur when the dam is subjected to seismic input. Compared to constraints on steady state response, constraints on transient response depend on one additional parameter: time. The constraints must be satisfied from the initial to some final time. For the actual computations, the constraints must be discretized at a series of time points. The distribution of time points has to be dense enough to preclude the possibilities of significant constraint violation between time points. This type of constraint discretization can greatly increase the number of constraints and thereby the cost of optimization. Therefore it is desirable to find ways to remove the time dependence without substantially increasing the number of constraints. The use of envelope functions is one approach to to reduce the number of constraints handled by the optimizer and making it more efficient.

Finding the optimum profile of the dam can then be posed as a multicriteria optimization problem in which all the constraints and objective function are folded in a single envelope. The entropy-based approach to solving this minimax optimization formulates the problem as the minimization of a convex function with just one control parameter. The user-specified parameter controls how close the envelope is to the original constraints and the objective function.

2. Problem Formulation

2.1 Shape Representation

The design of dams is fundamentally a configuration optimization problem where the external geometry of the structure is to be determined. Typically the number of actual design variables is small and in the case of gravity dams control nodes can be used to define the coordinates of the boundary nodes and their moving directions. The geometry of a concrete gravity dam shown in Figure 1 is described by 3 or 5 design (shape) variables.

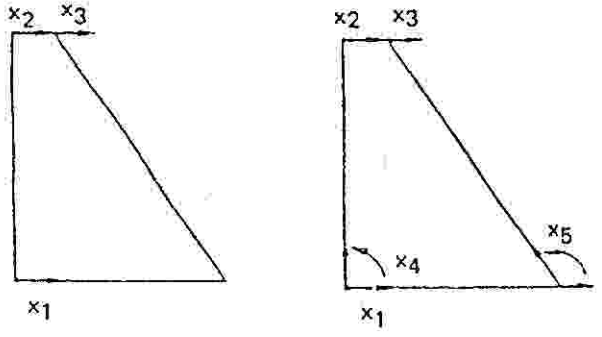

Shape Variables
Figure 1

x_1, x_2 and x_3 give the position of the cross section's bottom left, top left and top right, respectively, with respect to the starting shape of the dam. The position of the bottom right of the downstream face is fixed. x_4 and x_5 are the tangents at the bottom left and right of the heel, respectively. Although the upstream and downstream faces may have parabolic shapes if the last two design variables are used, the boundary is approximated by piecewise linear functions.

2.2 Static Analysis of the Structure

As the concrete gravity dam is subjected to static and dynamic loading conditions, a short summary of the relevant analysis technique will be presented next. The structural analysis consists of solving the equilibrium equations

$$K\,u = P \tag{1}$$

where K is the structural stiffness matrix, formed by assembling all elements stiffness matrices K_e, u is the unknown nodal displacement matrix and P the generalized load vector including self weight of the structure, hydrostatic pressure or thermal loads. Both K and P are functions of the shape variables x_i. Given the nodal displacements, a structural response R can be related to them through matrix Q:

$$R = Q\,u \tag{2}$$

The stress matrix at a given point can also be written as:

$$\sigma = S_e\,u_e \tag{3}$$

where Sc is the element stress matrix depending on the element nodal forces and on the element stiffness matrix; u_e is the element nodal displacements.

When the optimization requires function evaluation a complete finite element analysis is performed. However, because the actual configuration of the structure is changing, the finite element generated for the initial configuration may not be adequate throughout the design process. Therefore, it is necessary to provide automatic mesh generation capability within the finite element analysis program to ensure that the analysis results are always meaningfull. Because a detailed analysis is required at each step in the optimization process, the problem should be formulated to reduce computational effort. One attractive approach to this is to begin the design with a relatively coarse finite-element mesh. As the optimization progresses, the mesh is refined in areas of high stress concentration so that as the optimum is approached the f.e. model is detailed enough to ensure reasonable accuracy. The finite element idealization for the system shown in Figure 2 consists of 18 quadrilateral elements and 77 nodes, which provide 154 degrees of freedom (90 in the dam and 64 on the foundation).

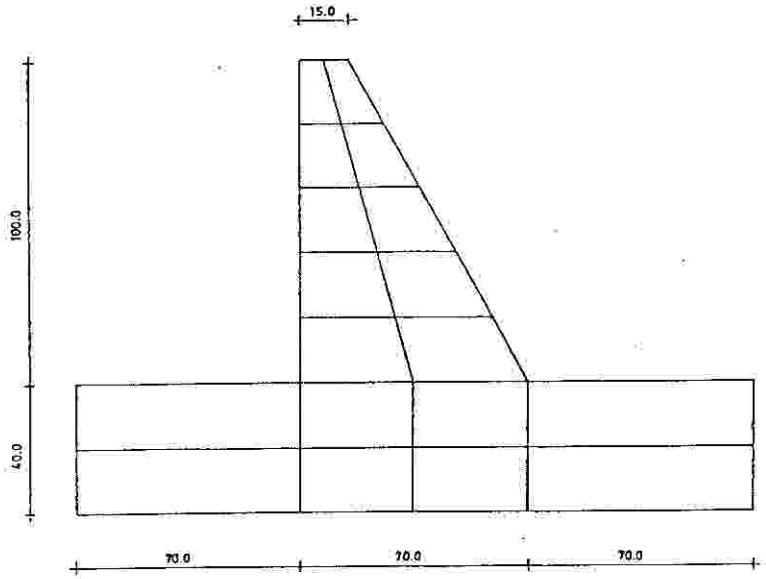

Finite Element Mesh

Figure 2

This mesh was refined to 72 quadrilateral elements (40 in the dam and 32 in the foundation) for the final shape to ensure that the response of the model was meaningfull.

2.3 Dynamic Response by Modal Analysis

The equations of motion at time t are:

$$M\ddot{u}(t) + C\dot{u}(t) + Ku(t) = P(t) \tag{4}$$

where M, C, and K are functions of time or constants in linear systems, while they are also functions of displacements, velocities, etc. in non-linear systems.

To facilitate the formulation of the explicit linear dynamic constraints for each design stage a modal superposition method is used to compute dynamic displacements and stresses. This analysis involves solving the system of undamped dynamic equilibrium equations that can be reduced to the eigenvalue equation:

$$K\Phi_r - \gamma_r M\Phi_r = 0 \tag{5}$$

where Φ_r is an eigenvector corresponding to the rth eigenvalue λ_r.
The expression for modal transformation is:

$$u = \Phi\, q \tag{6}$$

where Φ is the mode shape matrix and q is the general coordinate vector. Premultiplying equation (4) by the transpose of the rth eigenvector or mode-shape vector Φ_r leads to:

$$\phi_r{}^t M\phi\,\ddot{q} + \phi_r{}^t C\phi\,\dot{q} + \phi_r{}^t K\phi\, q = \phi_r{}^t P \tag{7}$$

The orthogonality conditions

$$\Phi_r M\Phi_s = 0 \quad r \neq s \tag{8a}$$

cause all components except the rth mode term in the mass and stiffness expressions in equation (7) to vanish.

$$\Phi_r K\Phi_s = 0 \quad r \neq s \tag{8b}$$

A similar simplification can be done for the damping expression if it is assumed thar the orthogonality conditions also apply to the matrix, i.e.

$$\Phi_r C\Phi_s = 0 \quad r \neq s \tag{8c}$$

We further normalize the eigenvalue ϕ_r such that:

$$\Phi_r M\Phi_r = 1 \tag{9}$$

Hence, equation (4) is reduced to uncoupled equations of motion of the form:

$$\ddot{q}_r + 2\,\xi_r\,\omega_r\,\dot{q}_r + \omega_r{}^2\, q_r = P_r \tag{10}$$

where $\xi_r\,\omega_r$ and P_r are given by:

$$\omega_r{}^2 = \lambda_r = \phi_r{}^t K\,\phi_r \tag{11a}$$

$$2\xi_r\,\omega_r = 2\mu_r = \phi_r{}^t C\,\phi_r \tag{11b}$$

$$P_r = \Phi_r{}^t P \tag{11c}$$

In practice, equation (10) will be written for l modes, where l ≤ m. The displacements u are calculated by use of equation (6), after substitution for q_r from:

$$q_r = 1/\omega_{r'} \int_0{}^T P_r(t)\exp\left[-\xi_r\omega_r(T-t)\right]\mathrm{sen}\left[\omega_{r'}(T-t)\right]\,dt \tag{12}$$

where,

$$\omega_{r'} = \omega_r\sqrt{1-\xi_r{}^2} \tag{13}$$

which corresponds to the solution of equation (10).

2.4 Step-by-step Integration Procedure

The step-by-step integration technique is suitable for both linear and non-linear systems. The response is evaluated for a series of short time increments, δt, generally taken of equal length for computational convenience. Among step-by-step integration techniques, Newmark's β method is widely used. Let all quantities in equation (4) be known at time t. The displacements and velocities at time $t+\delta t$ are assumed as follows:

$$u(t+\delta t) = u(t) + \delta\, t\dot{u}(t) + (1/2-\beta)\,\delta t^2\ddot{u}(t) + \beta\,\delta t^2\ddot{u}(t+\delta t) \quad (14a)$$

$$\dot{u}(t+\delta t) = \dot{u}(t) + \delta t/2\,[\ddot{u}(t) + \ddot{u}(t+\delta t)] \quad (14b)$$

where $0 \le \beta \le 1/6$. The time interval δt is generally selected to be about one-sixth of the shortest natural period of the system. Substitution of equations (14a-b) into equation (4) at the time $(t+\delta t)$ will give:

$$\ddot{u}(t+\delta t) = \left[M + \delta t/2C + \beta\delta t^2K\right]^{-1}\{P(t+\delta t) - C[\dot{u}(t) + \delta t/2\ddot{u}(t)] - K\left[u(t) + \delta t\dot{u}(t) + (1/2-\beta)\delta t^2\ddot{u}(t)\right]\} \quad (15)$$

2.5 Hydrodynamic pressures

The basic problem of hydrodynamic pressures on dams during earthquakes was first solved analytically by Westergaard in 1933 for vertical upstream faces. Chwang and Housner [15] extended the momentum balance method developed by Von Karman also in 1933 to obtain pressures on dams with inclined face. On the basis of the continuity of fluid flow, the equation of motion and boundary conditions, Yang [16] obtained a closed form solution. The corresponding nonlinear system of four equations with four unknowns can be solved iteratively. If the vertical component of the fluid acceleration is not required a solution can be found by using two coupled equations with two unknowns. Fig. 3 shows the variation of the hydrodynamic coefficients with respect to the front face angle.

A more accurate semi-analytical solution for hydrodynamic pressure destribution on dams with arbitrary upstream face is used here Tsai [17]. The compressibility of the water is included in the formulation. The pressure distributions in the fluid domain are expressed as the sum of functions with amplitude coefficients that satisfy all boundary conditions except at the upstream face of the dam. These coefficients are determed by using least squares (or Galerkin) so that the residual error is minimized.

3. Optimization

3.1 Multi-objective formulation

Pareto's economic principle is gaining increasing acceptance to multi-objective optimization problems. In minimization problems a solution vector is said to be "Pareto optimal" if no other feasible vector exists that could decrease one objective function without increasing at least another one. The optimum vector usually exists in practical problems and is not unique. The overall objective of concrete dam design is to achieve an economic and safe solution. In this study it is not intended to include all factors influencing the economics of a design. One of the factors conventionaly adopted is the concrete volume. The volume of the dam is the sum of the volumes of the finite elements,

$$V = \sum_e v_e \quad (16)$$

where e is the index of a finite element in the dam. A second set of goals arises from the requirement that the stresses should be as

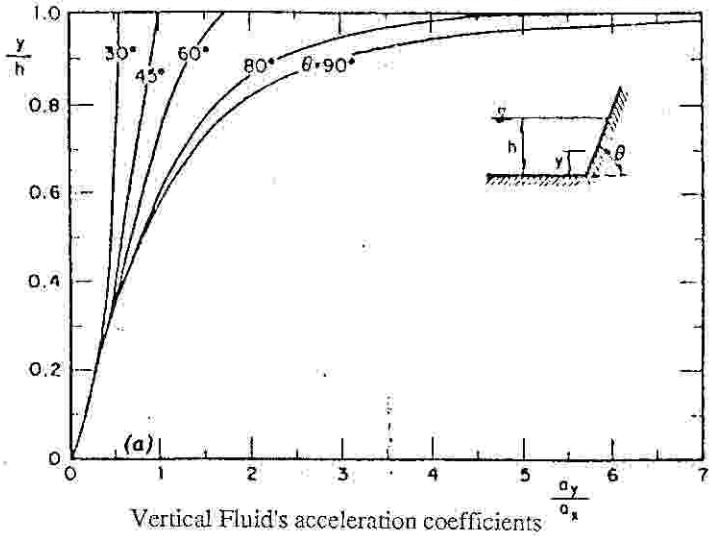

Vertical Fluid's acceleration coefficients

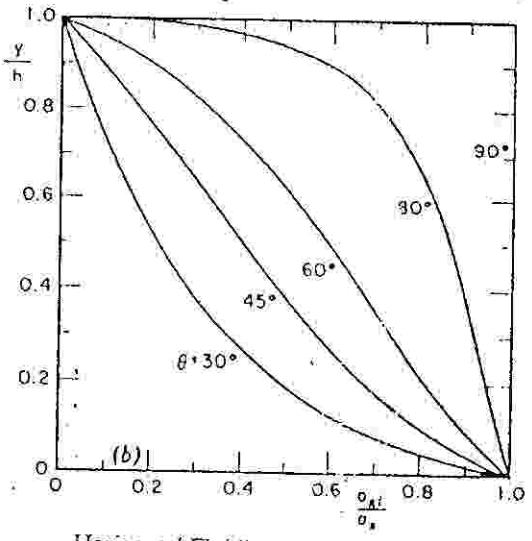

Horizontal Fluid's acceleration coefficients

Hydrodynamic coefficients versus Front Face Angle

Figure 3

small as possible:

$$\sigma(x) \le \sigma^u \qquad \sigma(x) \ge -\sigma^l \tag{17}$$

where su and sl are tensile and compressive admissible stresses, respectively. The stresses can be of any kind: normal, shear and principal stresses. A further goal comes from the imposition of stability against sliding. The following form is used:

$$c_1 F_h + c_2 F_v - c_o \le 0 \tag{18}$$

where c_o,c_1 and c_2 are constants and F_h, F_v are the global forces in the horizontal and vertical directions, respectively. Similarly, the global moment requirement is introduced to control the overturning moment:

$$c_3 [F_h (v-v_o) - F_v (h-h_o)] - c_4 b F_v \le 0 \tag{19}$$

where b is the thickness of the base, c_3 and c_4 are constants. v and h are coordinates of F_h and F_v, respectively. (h_o,v_o) are the coordinates of the point at the base of the dam on the downstream face, which is kept fixed during the optimization. On the basis of this expression it is possible to impose limits on the eccentricity of global forces:

$$e(x) \le e^u \qquad e(x) \ge -e^u \tag{20}$$

The crest of a dam must have substantial thickness to resist the shock of floating objects, to afford a roadway and to support auxiliary structures on the top of the dam.

$$l(x) \ge l^l \tag{21}$$

The optimization method described in the next section requires that all these goals should be casted in a normalized form.

If some reference volume $\underline{V}$ is specified, these criteria may be written in the form,

$$g_1(x) = \frac{V(x)}{\underline{V}} - 1 \le 0 \tag{22a}$$

$$g_2(x) = \frac{\sigma(x)}{\sigma^u} - 1 \le 0 \tag{22b}$$

$$g_3(x) = \frac{\sigma(x)}{\sigma^l} + 1 \le 0 \tag{22c}$$

$$g_4(x) = c_1 F_h(x) / c_o + c_2 F_v / c_o - 1 \le 0 \tag{22d}$$

$$g_5(x) = \frac{e(x)}{e^u} - 1 \le 0 \tag{22e}$$

$$g_6(x) = \frac{e(x)}{e^l} + 1 \le 0 \tag{22f}$$

$$g_7(x) = -\frac{t}{t^l} + 1 \le 0 \tag{22g}$$

The objective is to minimize all of these goals over shape variables x. This is achieved by solving the minimax optimization problem:

$$\mathrm{Min}_x \, \mathrm{Max}_j \, (g_1, ..., g_j ... g_7) = \mathrm{Min}_x \, \mathrm{Max}_{j=1,7} < g_j(x) > \tag{23}$$

Different weights can be attributed to different goals just by changing the reference volume, tiping moments, stress or eccentricity limits. The objective of this Pareto optimization is to obtain an unbiased improvement of the current design.

3.2 Minimax Optimization

The minimax problem (23) is discontinuous and non-differentiable, both of which attributes make its numerical solution by direct means difficult. Simões and Templeman [18] have shown that the minimax solution may be found indirectly by the unconstrained optimization of a scalar function which is both continuous and differentiable and thus considerably easier to solve. In this section some of the theory behind this approach to minimax optimization is briefly described.

For any set of real, positive numbers U_j, j=1, ..., J, and real $\rho \ge q \ge 1$, Jensen's inequality states that,

$$\left(\sum_{j=1,m} U_j^{\rho}\right)^{1/\rho} \le \left(\sum_{j=1,m} U_j^{q}\right)^{1/q} \tag{24}$$

Inequality (24) means that the p-th norm of the set U decreases monotonically as its order, p, increases. Another important property of the p-th norm is its limit as ρ tends towards infinity:

$$\lim_{\rho\to\infty}\left(\sum_{j=1,m} U_j^{\rho}\right)^{1/\rho} = \mathrm{Max}_{j=1,m} < U_j > \tag{25}$$

Consider the minimax optimization problem,

$$\mathrm{Min}_x \; \mathrm{Max}_{j=1,m} < g_j(x) > \tag{26}$$

and Jensen's inequality. Let $U_j = \exp [g_j(x)]$, j=1,...,m thus ensuring that $U_j > 0$, for all positive $g_j(x)$. Then,

$$\left(\sum_{j=1,m} U_j^{r}\right)^{1/\rho} = \left\{\sum_{j=1,m} \exp\left[\rho g(x)\right]\right\}^{1/\rho} \tag{27}$$

And from (25),

$$\lim_{\rho\to\infty}\left\{\sum_{j=1,m} \exp\left[\rho g(x)\right]\right\}^{1/\rho} = \mathrm{Max}_{j=1,m} < \exp\left[g_j(x)\right] > \tag{28}$$

Taking logarithms of both sides and noting that,

$$\log \lim(f) = \lim \log(f) \quad \text{and} \quad \log \mathrm{Max}(f) = \mathrm{Max} \log(f) \tag{29}$$

Eq.(28) becomes,

$$\lim_{\rho\to\infty}(1/\rho)\log\left\{\sum_{j=1,m}\exp\left[\rho g(x)\right]\right\} = \underset{j=1,m}{\mathrm{Max}} < g_j > (x) \qquad (30)$$

Result (30) holds for any set of vectors g(x), including that set which results from minimizing both sides of (26) over x. Thus (30) can be extended to:

$$\mathrm{Min}_x \underset{j=1,m}{\mathrm{Max}} < g_j(x) > = \mathrm{Min}_x(1/\rho)\log \left\{\sum_{j=1,m}\exp\left[\rho g_j(x)\right]\right\} \qquad (31)$$

with increasing ρ in the range $1 \le \rho \le \infty$. Result (31) shows that a Pareto solution of the minimax optimization problem can be obtained by the scalar minimization,

$$\mathrm{Min}_x(1/\rho)\log\left\{\sum_{j=1,m}\exp\left[\rho g_j(x)\right]\right\} \qquad (32)$$

with a sequence of values of increasingly large positive $\rho \ge 1$.

3.3 Scalar Function Optimization

Problem (32) is unconstrained and differentiable which, in theory, gives a wide choice of possible numerical solution methods. However, since the goal functions $g_j(x)$ do not have explicit algebraic form in most cases, the strategy adopted was to solve (32) by means of an iterative sequence of explicit approximation models. An explicit approximation can be formulated by taking Taylor series expansions of all the goal functions $g_j(x)$ truncated after the linear term. This gives:

$$\mathrm{Min}(1/\rho)\log\left\{\sum_{j=1,7}\exp\rho\left[g_j(x_o)+\sum_{i=1,N}\frac{\delta g_j(x_o)}{\delta x_i}(x_i - x_o)\right]\right\} \qquad (33)$$

Problem (33) is now an explicit approximation to problem (32) if values of all $g_j(x_o)$ and $\partial g_j(x_o)/\partial x_i$ are known numerically. Given such values (33) can be solved directly by any standard unconstrained optimization method. Solving (33) for particular numerical values of $g_j(x_o)$ and $\partial g_j(x_o)/\partial x_i$ forms only one iteration of the complete solution of problem (32). The solution vector x_1 of such an iteration represents a new design which gives new values for $g_j(x_1)$ and $\partial g_j(x_1)/\partial x_i$ to replace those corresponding to x_o. Iterations continue until changes in the design variables become small. The minimax optimization algorithm requires a sequence of positive values of ρ increasing towards infinity. Many different schemes are possible depending upon the particular sequence chosen the convergence rate and stability of the algorithm. One way of estimating a value for ρ is to iterate to that value that makes the objective function of problem (33) stationary with respect to ρ. It can be seen that ρ increases as the unfeasibility of the current design decreases; i.e. increasing ρ tends to enforce feasibility.

Since the objective function of this unrestricted optimization problem is differentiable, methods which uses gradients are more efficient to solve (33). Nevertheless, care has to be taken in the calculation of the objective function derivatives. If these are determined analytically they are given by a sum of combinations of exponential terms, being computationally expensive. In the example presented latter, a quasi-Newton algorithm was adopted. The strategy followed during the sequential minimization process in this work was to initially employ a fairly refined mesh in time domain to define the discretized parametric functions. After completion of the first entire optimization process, a more refined time mesh is used to test whether or not the the current design is feasible. The first complete optimization was performed using a mesh time interval equal to one-eight the fundamental period of the initial design. For the final refined mesh a time interval equal to one-eight the third mode period for the current design was employed. The determination of values for the derivatives of the goal functions is considered next.

4. Sensitivity Analysis

4.1 Semi-analytic Method

To formulate and solve the explicit approximation problem numerical values are required for all the goal functions and all their first derivatives with respect to the design variables x. The expressions for the analytic method of sensitivity calculation are:

$$\frac{\partial R}{\partial x_i} = \frac{\partial Q^t}{\partial x_i}u + Q^t\frac{\partial u}{\partial x_i} \qquad (34a)$$

$$\frac{\partial u}{\partial x_i} = -K^{-1}\frac{\partial K}{\partial x_i}u + K^{-1}\frac{\partial P}{\partial x_i} \qquad (34b)$$

where Q, U and K are functions of x and the obtaining of the expresssions for $\partial K/\partial x_i$ and $\partial Q/\partial x_i$ involves lengthy derivation. The semi-analytic method for the sensitivity analysis of the responses to static loading consists of the following steps:

1 - Given a proper step length vector $\Delta x_i = (0, 0,...,\Delta x_i,...,0)$, the difference approximation of pseudo-load vector Q_p is:

$$Q_p = \sum_{e\in E}\left(-K_e(x+\Delta x_i)u + Ke(x)u + P_e(x+\Delta x_i) - P_e(x)\right)/\Delta x_i \qquad (35)$$

where subscript e denotes the eth element and E is the set of elements related to the design variable x_i.

2. - Solve $\partial u/\partial x_i$ from,

$$\partial u/\partial x_i = K^{-1}Q_p \qquad (36)$$

3. - Determine the first-order approximation of displacement at design $x+\Delta x_i$,

$$u(x+\Delta x_i) \cong u(x) + \partial u / \partial x_i \Delta x_i \tag{37}$$

4.- Obtain the sensitivity of the response by local differences:

$$\partial R / \partial x_i \cong \left[R(x+\Delta x_i, u+\Delta u) - R(x,u)\right] / \Delta x_i \tag{38}$$

Eigenvalue sensitivity problems arising in vibration and buckling problems require a different class of solution methods from those used in static and dynamic response sensitivity analysis [19]. Given $\partial u(t) / \partial x_i$, the gradients of the responses can be computed by finite differences - steps 3 and 4 of the semi-analytic method.

4.2 Modal Analysis

In the case of gravity dams the eigenvalue problem (5) is guaranteed to have real distinct solutions. Moreover, a good approximation to the mode shape can be obtained with a relatively small number of terms. Therefore mode acceleration procedures Sutter et al. [20] are not required to improve convergence. The gradients of displacements can be obtained by differentiation of equation (7) with respect to x_i:

$$\frac{\partial u}{\partial x_i} = \frac{\partial}{\partial x_i} \sum_r q_r \phi_r = \sum_r q_r \frac{\partial \phi_r}{\partial x_i} + \frac{\partial q_r}{\partial x_i} \phi_r \tag{39}$$

But, to compute $(\partial q_r / \partial x_i)$, the quantities:

$$\frac{\partial \omega_r}{\partial x_i} = \frac{1}{2} \frac{\partial \lambda_r}{\partial x_i} - 2\mu_r \frac{\partial \mu_r}{\partial x_i} \left(\lambda_r - \lambda_r^2\right)^{-1/2} \tag{40a}$$

and,

$$\frac{\partial \omega_r}{\partial x_i} = \phi_r{}^t C \frac{\partial \phi_r}{\partial x_i} + \frac{1}{2} \phi_r{}^t \frac{\partial C}{\partial x_i} \tag{40b}$$

are needed. It will be noted that the calculation of gradients of the eigenvalues and the eigenvectors is indispensable for the evaluation of the right-hand sides of equations (39) through (40). These calculations are discussed next [21-22].

Differentiating both sides of eigenvalue equation (5) with respect to each variable x_i gives:

$$\left(K - \lambda_r M\right) \frac{\partial \phi_r}{\partial x_i} + \frac{\partial K}{\partial x_i} - \lambda_r \frac{\partial M}{\partial x_i} \phi_r - \frac{\partial \lambda_r}{\partial x_i} M \phi_r \tag{41}$$

Pre-multiplying equation (41) by $\Phi_r{}^t$ and making use of the symmetry of M and K leads to the calculation for gradients of eigenvalues:

$$\frac{\partial \lambda_r}{\partial x_i} = \phi_r{}^t \frac{\partial K}{\partial x_i} - \lambda_r \frac{\partial M}{\partial x_i} \phi_r \tag{42}$$

Let,

$$B = K - \lambda_r M \tag{43}$$

When all eigenvalues λ_r are different the rank of B will be (m - 1). This allows for the following partition of equation (5):

$$\begin{bmatrix} B_{11} & , & b_{12} \\ b_{12}{}^t & , & -b_{22} \end{bmatrix} \begin{bmatrix} \phi_{-r-1} \\ \phi_{r2} \end{bmatrix} = \begin{bmatrix} 0 \\ 0 \end{bmatrix} \tag{44}$$

where ϕ_{r2} is a single scalar quantity, and b_{12} is a column vector.

Differentiation of equation (44) with respect to xi gives:

$$\begin{bmatrix} \delta B_{11} / \delta x_i & , & \delta b_{12} / \delta x_i \\ \delta b_{12} / \delta x_i{}^t & & \delta b_{22} / \delta x_i \end{bmatrix} \begin{bmatrix} \phi_{r1} \\ \phi_{r2} \end{bmatrix} + \begin{bmatrix} B_{11} & , & b_{12} \\ b_{12}{}^t & & b_{22} \end{bmatrix} \begin{bmatrix} \delta \phi_{r1} / \delta x_i \\ \delta \phi_{r2} / \delta x_1 \end{bmatrix} = \begin{bmatrix} 0 \\ 0 \end{bmatrix} \tag{45}$$

Equation (45) can be solved for $(\partial \phi_r / \partial x_i)$ in terms of the scalar $\partial \phi_{r2} / \partial x_i$:

$$\frac{\partial \phi_r}{\partial x_i} = \frac{\partial \phi_{r2}}{\partial x_i} a + A_i \phi_r \tag{46a}$$

where,

$$a = \begin{bmatrix} -B_{11}{}^{-1} b_{12} \\ b_{22}{}^{-1} \quad b_{12}{}^t B_{11}{}^{-1} b_{12} \end{bmatrix} \tag{46b}$$

and,

$$A = \begin{bmatrix} -B_{11}{}^{-1} \partial B_{11} / \partial x_i \\ b_{22}{}^{-1} \left(-\partial b_{12} / \partial x_i{}^t + b_{12}{}^t B_{11}{}^{-1} \partial B_{11} / \partial x_i\right) \\ -B_{11}{}^{-1} \partial b_{12} / \partial x_i \\ b_{22}{}^{-1} \left(-\partial b_{22} / \partial x_i + b_{12}{}^t B_{11}{}^{-1} \partial b_{12} / \partial x_i\right) \end{bmatrix} \tag{46c}$$

Therefore it is now necessary to determine the scalar quantity $(\partial \phi_{r2} / \partial x_i)$. To this end, equation (9) is first differentiated with respect to x_i:

$$\phi_r{}^t M \, \partial \phi_r / \partial x_i + \phi_r{}^t \partial M / \partial x_i \, \phi_r = 0 \tag{47}$$

By substitution of equation (46a) into equation (47), and rearrangement:

$$\frac{\partial \phi_{r2}}{\partial x_i} = \frac{2 \phi_r{}^t M A_i \phi_r + \phi_r{}^t \partial M / \partial x_i \, \phi_r}{2 \phi_r{}^t M a} \tag{48}$$

Finally, from equation (46a):

$$\frac{\partial \phi_{r1}}{\partial x_i} = -B_{11}{}^{-1} \left[\frac{\partial B_{11}}{\partial x_i} \phi_{r1} + \frac{\partial b_{12}}{\partial x_i} \phi_{r2} + b_{12} \frac{\partial \phi_{r2}}{\partial x_i} \right] \tag{49}$$

4.3 Step-by-step Integration Procedure

The gradients of the accelerations can be computed by differentiation of equation (15) with respect to each design variable x_i. Rearranging the resulting expression, one obtains:

$$\partial\ddot{u}(t+\partial t)/\partial x_i = \left[M+\delta t/2C+\beta\,\delta t^2K\right]^{-1}$$
$$\left\{A_1u(t)+A_2\dot{u}(t)+A_3\ddot{u}(t)+K\frac{\partial u(t)}{\partial x_i}+\right.$$
$$\left.A_4\frac{\partial\dot{u}(t)}{\partial x_i}+A_5\frac{\partial\ddot{u}(t)}{\partial x_i}+A_6\ddot{u}(t+\delta t)\right\} \qquad (50)$$

where,

$A_1=\partial K/\partial x_i;\quad A_2=\partial C/\partial x_i+\delta t\partial K/\partial x_i$

$A_3=\delta t/2\partial C/\partial x_i+(1/2-\beta)\delta t^2\partial K/\partial x_i;$

$A_4=C+\delta tK\quad A_5=\delta t/2\partial C+(1/2-\beta)\delta t^2K;$

$A_6=\partial M/\partial x_i+\delta t/2\partial C/\partial x_i+\beta\delta t^2\partial K/\partial x_i$

Equation (50) can be directly used for computation of the sensitivities. In fact, since the displacements and velocities can be found by substitution of equation (15) into equations (14a) and (14b), respectively, the gradients for these quantities can also be obtained by direct differentiation with respect to each design variable x_i. Thus, for example, for the velocities, one will obtain:

$$\partial\dot{u}(t+\delta t)/\delta x_i=\delta/\delta x_i\left\{\dot{u}(t)+\delta t/2\left[\ddot{u}(t)+\ddot{u}(t+\delta t)\right]\right\} \qquad (51a)$$

Similarly, the gradients for the displacements can be found by using:

$$\partial u(t+\delta t)/\delta x_i=\delta/\delta x_i$$
$$\left\{u(t)+\delta t\dot{u}(t)+(1/2-\beta)\delta t^2\ddot{u}(t)+\beta\delta t^2\ddot{u}(t+\delta t)\right\} \qquad (51b)$$

It will be noted that the calculation of the derivatives of the accelerations and velocities is indispensable for the evaluation of the displacement sensitivities.

5. Example

The following problem is chosen to illustrate the optimization procedure [4] for static loading. The dam is 100 m height and has 6 m minimum thickness. The compressive and tensile strengths of the concrete are 10,000 kN/m^2 and 1,000 kN/m^2, respectively. Elastic properties:

E=2.1 10^7 kN/m^2 ; ν = 0.2 ; body forces 2.4 10^7 kN/m^2

Foundation properties:

E = 10^7kN/m^2 ; ν = 0.15

The load combinations are: 1) dead weight; 2) self weight, water pressure, uplift; 3) dead weight, water pressure, uplift, earthquake; 4) dead weight, earthquake.

The safety factor for load conditions 1) and 2) is 2.5. The tensile stresses in the air and water faces are 400 kN/m^2 and hγ-400 $\leq$ 0, respectively, where h is the weight below water and γ is the unit water weight. Safety against sliding is guaranteed if V 0.8/H $\geq$ 1.5, where V and H are the sums of vertical and horizontal forces, respectively. Safety against overturning requires that the eccentricity of the resulting force e be |e| $\leq$ 1/6.

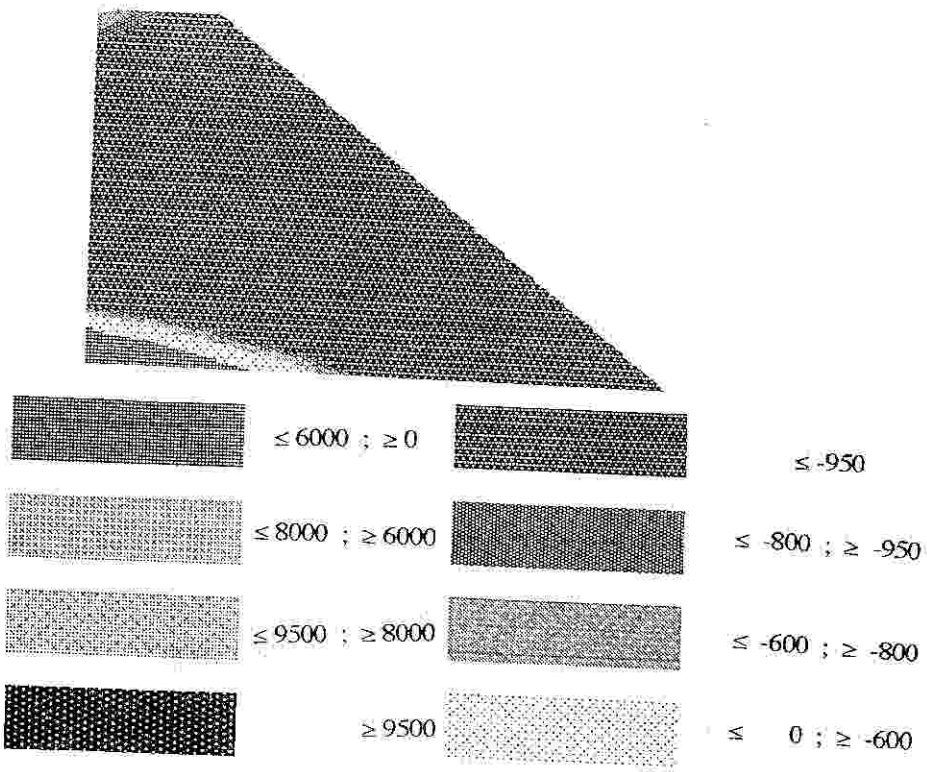

MAXIMUM TENSILE STRESSES
Figure 4

The safety factor for load conditions 3) and 4) is 1.92. The tensile stresses in the air and water faces are 520 kN/m^2 and $h\gamma - 520 \leq 0$, respectively. Safety against sliding is guaranteed if $V\ 0.8/H \geq 1.2$. Safety against overturning requires that the eccentricity e should be $|e| \leq 1/3$. Energy dissipation in the structure is represented by constant hysteretic damping. An equivalent damping ratio of 0.05 is considered.

The seismic effects are computed by standard static forces and dynamic analysis. Fig.4 represents the maximum tensile stresses that arise during an earthquake when the initial shape is considered. This shape is inadequate because the tensile stresses largely exceed their allowable values.

Sliding, overturning and minimum thickness at the top are the critical goals in the static approach. This design fails to predict the large tensile stresses that arise in the downstream face. Tensile stresses 2.5 times larger than the allowable values were found when the static optimal shape was analysed by the linear dynamic routine. Consequently stress requirements are critical in finding optimal shapes on the basis of linear dynamic behaviour. Moreover, these tensile stresses cause a large increase of concrete volume. Fig.5 shows the shapes and corresponding maximum tensile stresses obtained for the linear dynamic approach after 1 and 3 iterations, respectively, for the 3 and 5 variable representation.

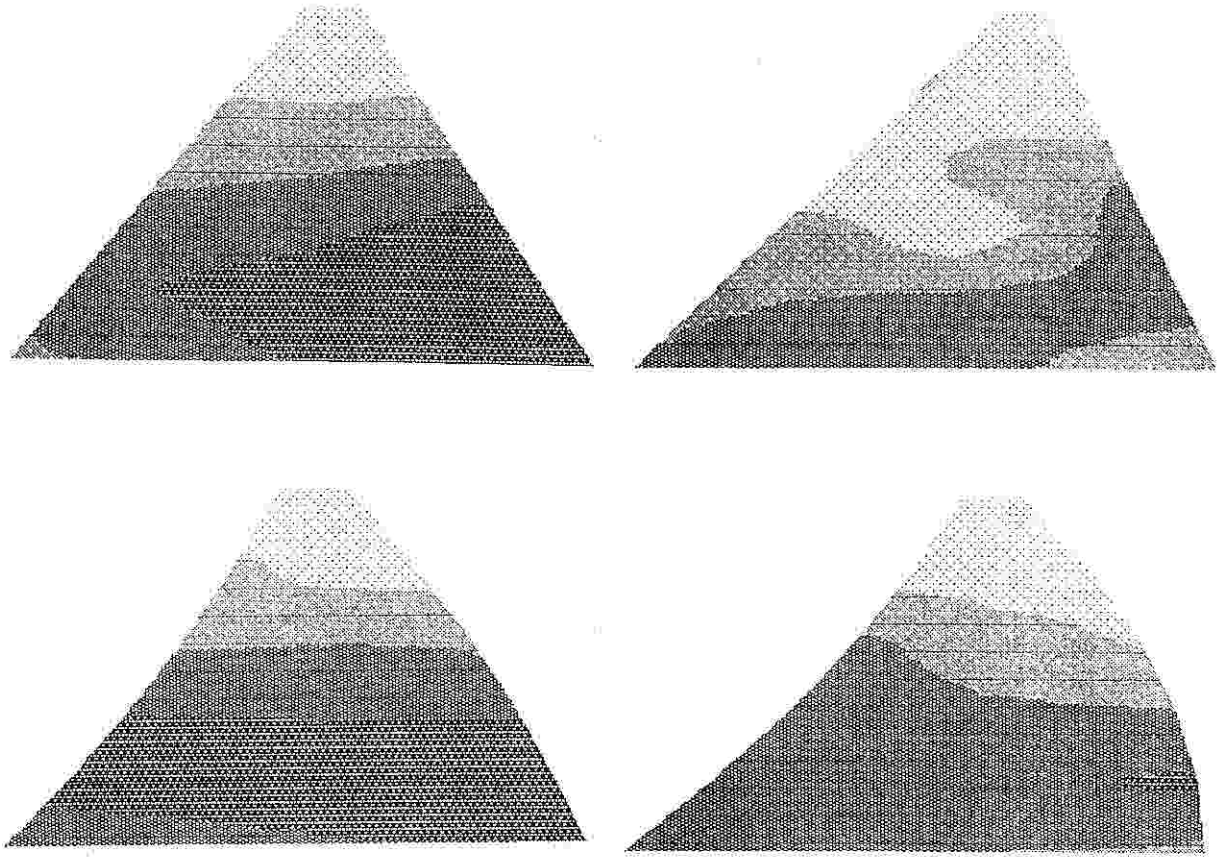

Figure 5

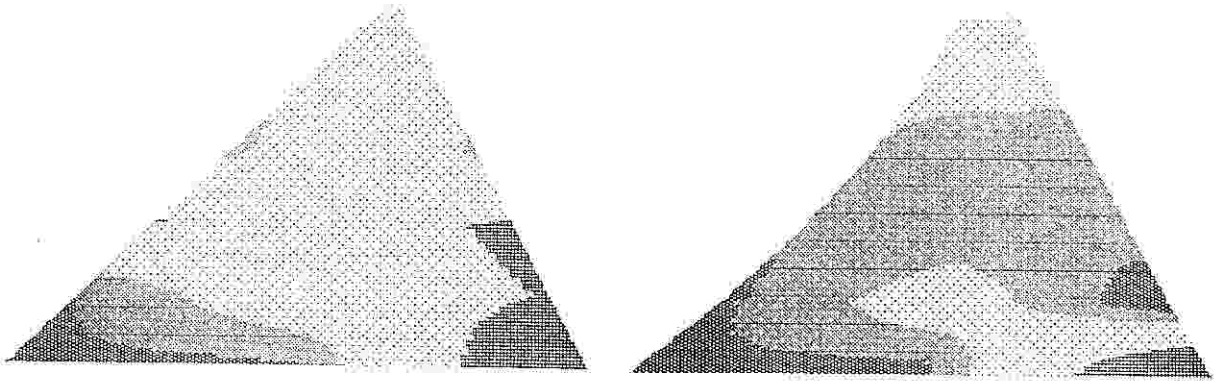

Figure 6

Fig. 6 represents the solution obtained after 2 iterations when a elastoplastic Mohr-Coulomb yield criteria is used to model the concrete behaviour. The elastoplastic model gives a more economical design by reducing the concrete volume by approximately 13%.

The optimal geometries are shown in Figure 7. Due to increasing flexibility of describing the shape of the dam, the volume may be reduced by increasing the number of design variables. The volume reduction is due to the increase in the vertical component of water pressure.

response of concrete gravity dams. Maximum tensile stresses in the air face are dominant when the dynamic response is considered. These tensile stresses cause a substantial increase in concrete volume. Nevertheless the concrete volume can be reduced by using a nonlinear model.

The contributions of the vertical component of ground motion to the response of concrete gravity dams are significant because, even though the ground motion is in the vertical direction, hydrodynamic pressures act in nearly the horizontal direction on a nearly vertical upstream face, causing lateral response. For low

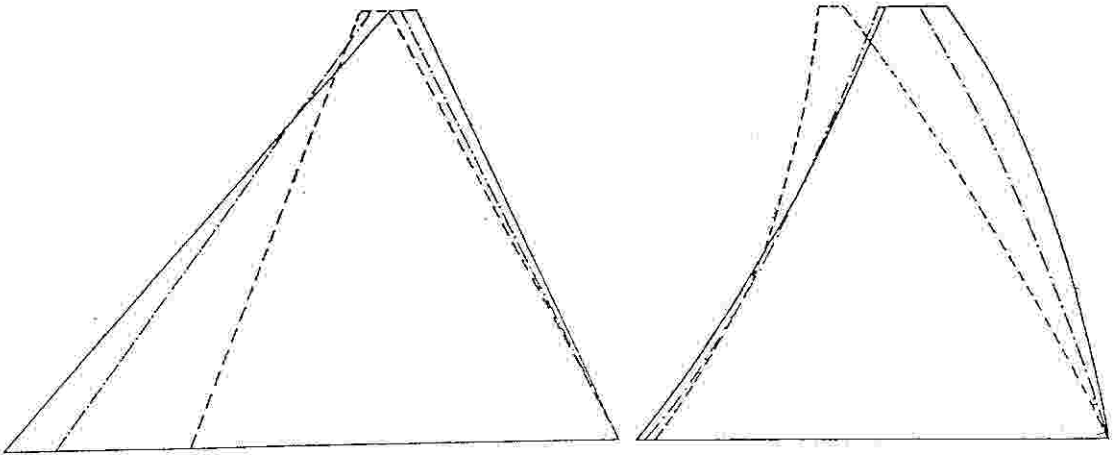

----- static solution

——— linear dynamic solution

———— nonlinear dynamic solution

Optimal Geometries

Figure 7

6. Discussion and Conclusions

The proposed design method consits of the combination of two algorithms: an implicit-explicit step-by-step integration procedure for the analysis and an optimization module. Sensitivity analysis is based on the dynamic procedure employed and provides the link between these two.

An optimal set of shape variables is found by minimizing a group of objectives. A minimax solution is obtained by the scalar minimization of a convex function involving one control parameter.

The standard design loadings for gravity dams include water pressure in addition to hydrostatic pressure associated with earthquakes. The additional water pressures associated with horizontal earthquake motion in the standard design loads, based on assumptions of rigid dam and incompressible water, underestimate the importance of the hydrodynamic effects in the height dams, the response to the vertical component of ground motion is especially significant; it can even exceed the response to the horizontal component. For dams of moderate to large height, the response to vertical ground motion, although smaller than that due to the horizontal components, may be significant.

Acknowledgement

The author wish to thank the financial support given by JNICT (Junta Nacional de Investigação Científica e Tecnológica, Projecto STRDA/C/TPR/576/92).

References

1. Zienkiewicz, O.C. and Campbel, J.S. (1973): Shape Optimization and Sequential Linear Programming. In: Gallagher, R.H. and Zienkiewicz, O.C. (Ed.):Optimum Structural Design, 109-126, J.Wiley.

2. Ramakrishnan,C.V. and A. Francavilla (1975): Structural Shape Optimization using Penalty Functions. J.Struct. Mech. 3, 403-422.

3. Vitiello, E. (1973): Shape Optimization using mathematical Programming and Modelling Techniques. Second Symposium on Structural Optimization, AGARD Conf. Poc. CP-123, Milan, Italy.

4. Wassermann, K. (1983-84): Three Dimensional Shape Optimization of Arch Dams with prescribed Shape Functions. J. Struct. Mechanics 11, 465-489.

5. Ricketts, R.E. and Zienkiewicz, O.C. (1984): Shape Optimization of Continuum Structures. In: E. Atrek, R.H. Gallagher, K.M. Ragsdell and O.C. Zienkiewicz (Ed.): New Directions in Optimum Structural Design, 139-166,J.Wiley.

Chopra, A.K. (1978): Earthquake Resistant design of Concrete Gravity Dams. J. Struct Div. ASCE. 104, 964-971

7. Chopra, A.K. and Chakrabarty, P. (1981): Earthquake Analysis of Concrete Gravity Dams including Dam-water-foundation Rock Interaction. Earth. Engrg. Struct. Dynamics 9, 363-383.

8. Fenves, G. and Chopra, A.K. (1987): Simplified Earthquake Analysis of Concrete Gravity Dams: Separate Hydrodynamic and Foundation Interaction Effects. J. Engrg. Mechanics ASCE 111, 715-756.

10. Haftka, R.T. and Adelman, H.M. (1989): Recent Developments in Structural Sensitivity Analysis. Struct. Optimization 1, 137-151.

. Rubin C.P. (1970): Minimum Weight Design of Complex Structures subjected to a Frequency Constraint. AIAA Journal 8, 923-927.

12. Haftka, R.T. (1972): Automated Procedure for Design of Wing Structures to Satisfy Strength and Flutter Requirements. NASA TND-6534, Washington DC

13. Cassis, J.H. and Schmit, L.A. Jr. (1976): Optimum Structural Design with Dynamic Constraints. J. Struct. Div. ASCE 102, 2053-2071.

14. Mills-Curran, W.C. and Schmit, L.A. Jr (1983): Structural Optimization with Dynamic Behaviour Constraints. Proc. AIAA/ASME/ASCE/AHS 24th Structures, Structural Dynamics and Materials Conference, Lake Tahoe, 369-382.

15. Chwang, A.T. and Housner, G.W. (1978): Hydrodynamic Pressures on Sloping Dams during Earthquakes. Part1. Momentum Method. J. Fluid Mechanics 87, 335-341.

16. Yang,C.Y., Chen,S., Wang,H and Sanchez-Sesma,F.J (1979): Hydrodynamic Pressures on Dams with inclinec Face. J. Engrg. Mechanics Div. ASCE. 105, 717-722

17. Tsai, C.S. (1992): Semi-Analytical Solutions fo: Hydrodynamic pressure on Dams with Arbitrary Upstream Face Considering Water Compressibility. Comp. Structures 42, 497-502.

18. Simões, L.M.C. and Templeman, A.B. (1989): Entropy-based Synthesis of Pretensioned Cable Net Structures. Engrg. Optimization 15, 121-140.

19. Yamakawa, H. (1984): Optimum Structural Design for Dynamic Response. In: E. Atrek, R.H. Gallagher, K.M. Ragsdell and O.C. Zienkiewicz (Ed.): New Directions in Optimum Structural Design, 249-266,J.Wiley.

20. Sutter, T.R. and Camarda, C.J., Walsh J.L. and Adelman, H.M. (1988): A Comparison of Several Methods for the Calculation of Vibration Mode Shape Derivatives, AIAA Journal 26,1506-1511.

21. Fox, R.L. and Kapoor, M.P. (1970): Structural Optimization in the Dynamic Response Regime: A Computational Approach. AIAA Journal 8, 1798-1804.

22. Nelson, R.B. (1976): Simplified Calculation of Eigenvector Derivatives, AIAA Journal 14, 1201-1205.